

## Cathodic corrosion: Part 2. Properties of nanoparticles synthesized by cathodic corrosion

A.I. Yanson and Yu.I. Yanson

*Leiden Institute of Chemistry, Leiden University, Postbus 9502, Leiden 2300RA, The Netherlands*

E-mail: a.yanson@chem.leidenuniv.nl

Received November 16, 2012

We demonstrate how cathodic corrosion in concentrated aqueous solutions enables one to prepare nanoparticles of various metals and metal alloys. Using various characterization methods we show that the composition of nanoparticles remains that of the starting material, and the resulting size distribution remains rather narrow. For the case of platinum we show how the size and possibly even the shape of the nanoparticles can be easily controlled by the parameters of corrosion. Finally, we discuss the advantages of using the nanoparticles prepared by cathodic corrosion for applications in (electro-)catalysis.

PACS: 82.45.Aa Electrochemical synthesis;  
82.45.Jn Surface structure, reactivity and catalysis;  
82.45.Yz Nanostructured materials in electrochemistry;  
**82.65.+r** Surface and interface chemistry; heterogeneous catalysis at surfaces.

Keywords: cathodic corrosion, electrochemistry, nanoparticles, alloys.

### Introduction

In recent decades the interest in nanometer-sized particles, i.e. nanoparticles, of different materials has grown tremendously from both the fundamental and the application points of view. The reasons for such great interest are manifold. From the fundamental perspective, the reduction of the size of particles results in the change of their physical and chemical properties due to the mesoscopic and quantum mechanical effects. From the practical point of view, nanometer-sized particles are attractive due to their large surface-to-volume ratio. Both effects are actively explored in heterogeneous catalysis [1], where a process occurs at the surface of a (mostly noble metal) catalyst. The use of smaller, nanometer-sized particles therefore allows reducing the amount of catalyst needed for the reaction. Although much progress has been made in the development of reliable methods of nanoparticle synthesis, the lack of a universal and simple production method remains to be the bottleneck for their industrial application in many areas.

In the first part of this paper we have shown that cathodic corrosion may lead to the formation of metallic (platinum) nanoparticles. Here we present our further study on their properties, and explore the possibilities of applications for cathodic corrosion as a universal yet simple nanoparticle synthesis method. We show that not only platinum, but all tested metals are subject to cathodic corrosion which leads

to the formation of nanoparticles, whose size and perhaps even shape can be easily controlled. Additionally, we find that alloy nanoparticles of tunable composition can be easily produced using the cathodic corrosion method. While many possibilities of this versatile technique remain yet to be explored, the results presented here show that this method is quick, clean, “green” and versatile enough to warrant further investigation into possibilities for applications.

### Experimental details

Unless noted otherwise, nanoparticles were prepared in a small volume (10 ml) of a freshly-prepared NaOH solution in 18.2 M $\Omega$ -cm ultrapure water (MilliQ). A wire electrode of the desired material was submerged to a predefined depth and an ac voltage was applied to it, using glassy carbon as a counter electrode, until complete dispersion of the submerged wire. After the desired amount of nanoparticles was produced, the electrolyte was washed off by repeatedly centrifuging, decanting and re-dispersing in ultrapure water until the conductivity of the suspension dropped below 1  $\mu$ S/cm. By controlling the initial amount of cathodically corroded metal we could determine the mass concentration of the nanoparticles in suspension, and thus use a known weight amount of nanoparticles for further experiments. This aqueous suspension of nanoparticles was then drop-cast on different supports for further characterization with transmission electron microscopy (TEM), x-ray diffraction (XRD), and cyclic voltammetry (CV).

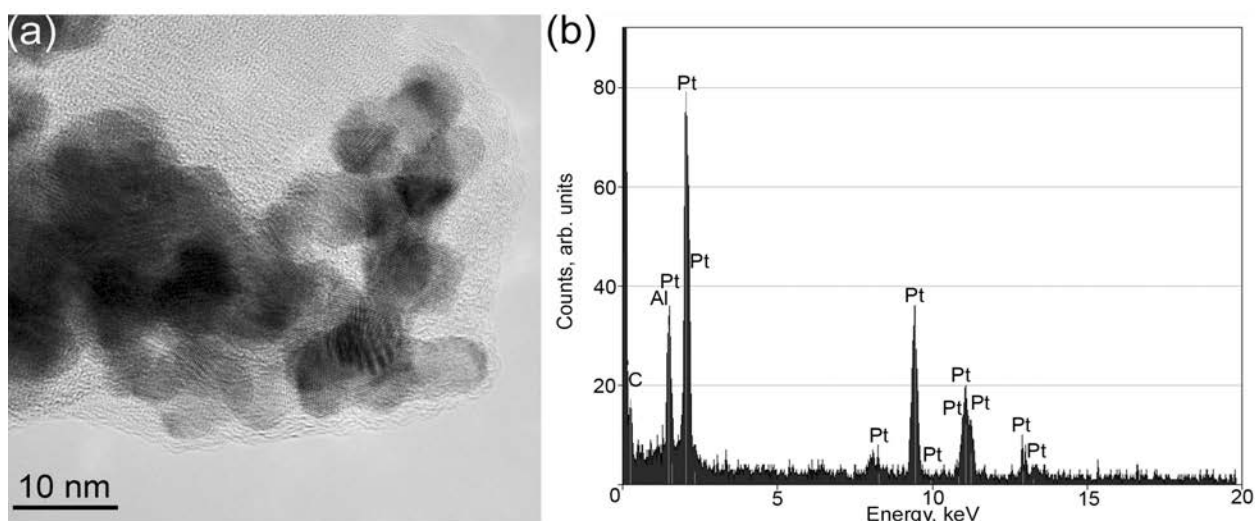


Fig. 1. (a) TEM image of Pt nanoparticles synthesized by cathodic corrosion. The corresponding EDX analysis graph is shown in (b). The EDX results show that the nanoparticles consist of pure metal. The weak signal of Al in the EDX spectrum comes from the TEM sample holder.

X-ray powder diffraction was performed on a Philips X'pert diffractometer, equipped with an X'celerator detector, in a  $\theta$ - $2\theta$  configuration. For XRD measurements, nanoparticles were drop-cast on a zero-background sample holder (Si or quartz). For the TEM measurements, Quantifoil<sup>tm</sup> carbon-on-copper grids were used in a FEI Tecnai F20 microscope. Electrochemical characterization of the nanoparticles was performed in a standard three-electrode glass cell, with the platinum flag used as a counter electrode and a reversible hydrogen electrode (RHE) as a reference electrode. A polished polycrystalline gold electrode, onto which a controlled amount of nanoparticles was drop-cast, was used as a working electrode. Potential was controlled by an Ivium (CompactStat) potentiostat. The electrolyte was prepared from Merck UltraPur<sup>tm</sup> reagents and ultrapure water, and thoroughly deaerated by bubbling with 5N argon for 15 min prior to each experiment.

#### Physical properties of nanoparticles prepared by cathodic corrosion

Figure 1(a) shows TEM images of Pt nanoparticles that were produced using the cathodic corrosion method. These nanoparticles were synthesized in a 10 M solution of NaOH using an ac voltage of  $-10$  to  $+10$  V as described in Part 1 [2]. From the lattice spacing in the TEM images, as well as from the energy dispersive x-ray (EDX) analysis in Fig. 1(b), we conclude that the particles consist of a pure metal. Hence, we conclude that cathodic corrosion has transformed the metallic wires into metallic nanoparticles.

Focussing on platinum, we have studied the particle size distribution by TEM. Figure 2 shows the distribution, whose maximum correlates well with the estimate for the average particle size of 12 nm obtained by fitting the widths of the XRD diffraction lines with the Scherrer for-

mula. The latter correlates the broadening of an XRD peak to the size of nanoparticles [3].

As one can see, the distribution is rather narrow and invites the question whether size controlled synthesis of nanoparticles is possible via this cathodic corrosion method. Figure 3(a) demonstrates that this is indeed the case. We have obtained XRD patterns of platinum nanoparticles synthesized at various current densities, and used Scherrer equation to determine the average particle size. The resulting semi-linear dependence shows that simply by varying the ac current during cathodic corrosion one can directly influence the size of the resulting nanoparticles between 6 and 12 nm.

An important measurement supporting the validity of this method of size determination via XRD is presented in Fig. 3(b). It is well-known that while the nanoparticles become smaller, their lattice constant decreases. By fitting the x-ray diffraction peaks we can determine their exact positions, and hence the lattice constant. The monotonous

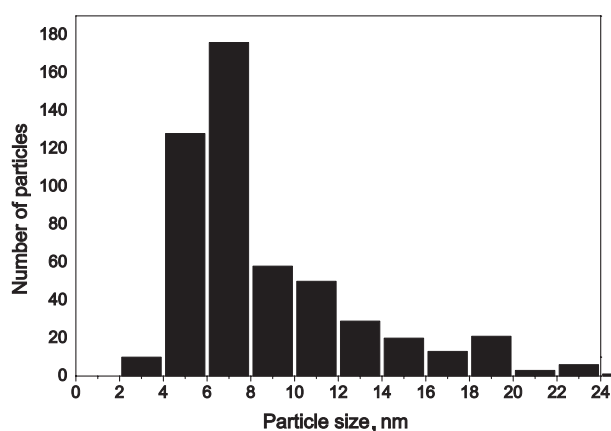


Fig. 2. Size distribution of platinum nanoparticles obtained by the ac cathodic corrosion in 10 M NaOH, as measured by the high-resolution TEM.

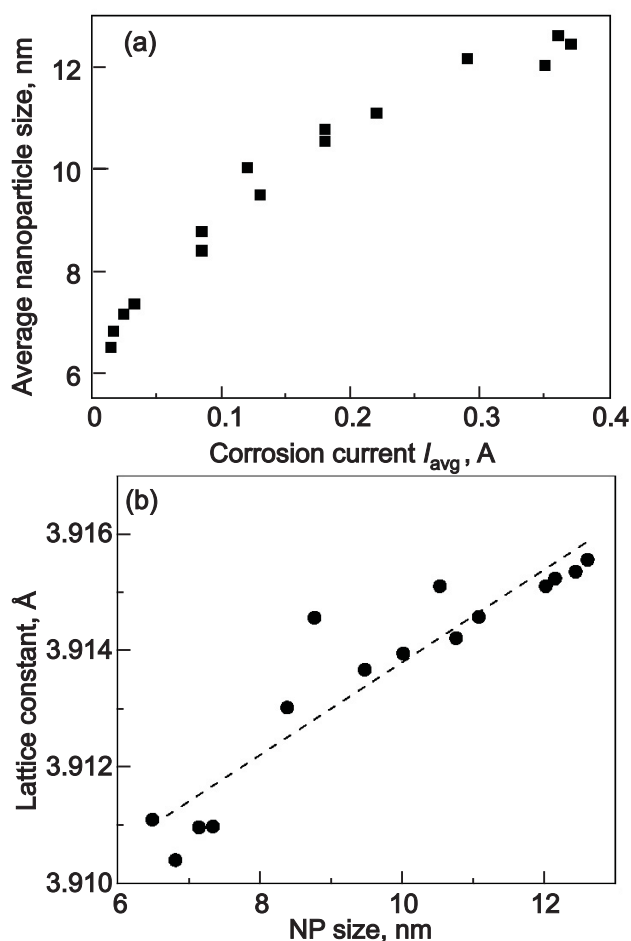


Fig. 3. (a) Nanoparticle size determined from the (111) XRD peak, using the Scherrer formula, as a function of the ac current employed during synthesis at  $-10$  to  $10$  V in a  $5$  M NaOH solution. (b) Average lattice constant determined from the position of the first five XRD lines for each nanoparticle sample using Bragg's law (bulk Pt value  $3.92$  Å).

contraction of the lattice constant for smaller nanoparticles, shown in Fig. 3(b), is in line with the reported values for particles of such sizes [4,5] indicating that our size determination is correct and that we have indeed achieved size-controlled synthesis with this method.

The dependence in Fig. 3(a) can be understood if we consider the model of cathodic corrosion presented in Part 1 of this article [2]. By increasing the current density we increase the corrosion rate and thus the concentration of the precursor for nanoparticle growth in the electrolyte adjacent to the electrode. In the nucleation-and-growth mechanism, such increase would lead directly to the formation of larger nanoparticles under the assumption that the nucleation density remains constant. This is indeed what we observe.

Many properties of nanoparticles are governed by the fact that a significant fraction of the atoms are on the surface. As the surface tension of such high curvature objects is rather high, the system usually tries to minimize the sur-

face area by adopting a quasi-spherical shape. However, many interesting properties arise if one can coerce the nanoparticles into some peculiar, nonequilibrium shapes [6]. A distinct plasmon resonance in gold nanorods is perhaps the most prominent example of the usefulness of these properties [7]. Here we show that using our synthesis method we can influence the surface properties of nanoparticles, creating particles with a large fraction of (100) facets at the surface. Such particles with relatively open surfaces are very promising nanocatalysts [8]. In Fig. 4 we present a TEM image of such nonspherical particles and a set of the so-called "blank" cyclic voltammograms, which show the hydrogen desorption region on platinum nanoparticles prepared in different concentrations of NaOH. A clear tendency of the increase of the peak at  $0.27$  V and the

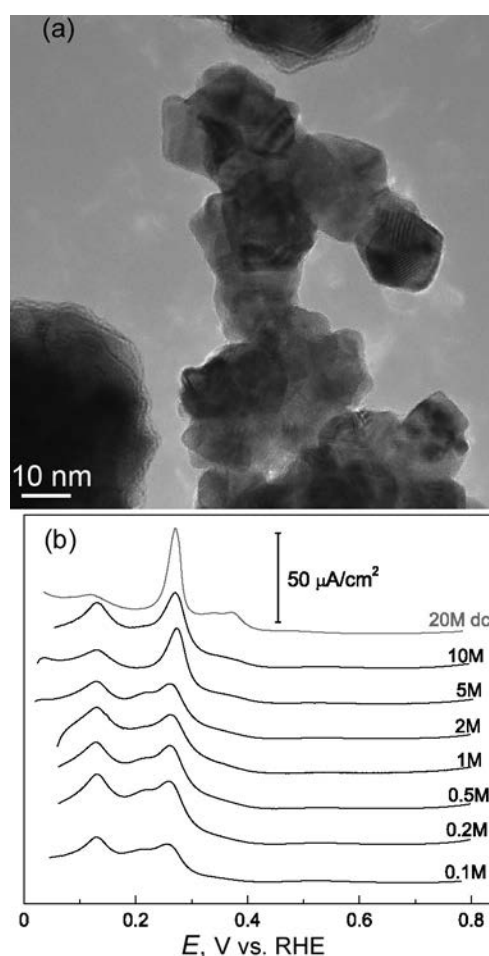


Fig. 4. (a) TEM images of nonspherical platinum nanoparticles prepared by ac corrosion in  $10$  M NaOH. (b) Cyclic voltammograms (CVs) of  $5 \mu\text{g}$  of platinum nanoparticles synthesized in various concentrations of NaOH electrolyte at  $-10$  to  $+10$  V ac (black) and at  $-10$  V dc (grey). Particles were drop-cast on a gold support and the CVs were measured in hanging meniscus configuration in a three-electrode electrochemical cell. The cell was filled with  $100$  ml of  $0.5$  M  $\text{H}_2\text{SO}_4$  solution, de-aerated with argon of  $5\text{N}$  purity. Curves were recorded at  $50$  mV/s scan rate and normalized by the electrochemical surface area using the  $210 \mu\text{C}/\text{cm}^2$  coefficient from Ref. 13.

formation of a shoulder at 0.36 V with increasing concentration can be seen. Comparing with the reference voltammograms for platinum single crystals [9] we conclude that our nanoparticles develop more and more (100) step and terrace sites at their surface. Following the analysis of Ref. 10 we see that for the nanoparticles prepared in most concentrated electrolytes, the amount of (100) sites at the surface exceeds 50%.

The fact that the preferential orientation of the surface of the nanoparticles can be influenced just by the concentration of the solution, in which the nanoparticles are synthesized, is rather unique. In general, to change the shape of nanoparticles that are produced by conventional chemical reduction methods, additional substances that adsorb preferentially on certain crystallographic planes are added to the solution. The growth of these planes can be either inhibited or promoted by the adsorption, leading to either stronger or weaker expression of these planes on the surface of the particles, correspondingly. However, these adsorbed additives also act as “contaminants”, inhibiting the useful properties of such nanoparticles during catalysis. These additives adsorb so strongly that they are difficult to remove from the particle surface [11]. In order to explain our shape-selective synthesis without additives, we suggest that the cations ( $\text{Na}^+$ ) that are present in the solution are preferentially adsorbed on the (100) crystallographic planes,

thus leading to a stronger expression of these planes on the nanoparticles. In fact, recent DFT calculations have confirmed that adsorption of  $\text{Na}^+$  is energetically much more favorable on the (100) planes of platinum [12]. The advantage of this method to control the preferred orientation of the surface of the particles is that the surface remains clean, i.e., free of adsorbed organics.

The mechanism of cathodic corrosion that we have proposed in the first part of this paper does not rely on the particular type of cationic species present in solution, as long as the cation remains irreducible at the electrode surface. We have confirmed experimentally that cathodic synthesis of nanoparticles proceeds in solutions containing  $\text{Li}^+$ ,  $\text{K}^+$ ,  $\text{Cs}^+$ ,  $\text{Ca}^{2+}$ , as well as ammonium and tetraalkylammonium cations. Moreover, nanoparticles are formed during cathodic corrosion in solutions rather independent of the type of the anions [14]. The generic nature of this phenomenon suggests applicability to metals other than platinum. Indeed, we have observed cathodic corrosion and nanoparticle formation for Pt, Rh, Pd, Au, Cu, Re, Fe, Ni, Nb, Ti, Si and Al. While for some the particles remain metallic, for others, due to the aqueous alkaline environment in which they are formed, they quickly oxidize. This demonstrates that the cathodic corrosion method can be used to produce nanoparticles of virtually any metal. Characterization of some metallic particles is shown in Fig. 5.

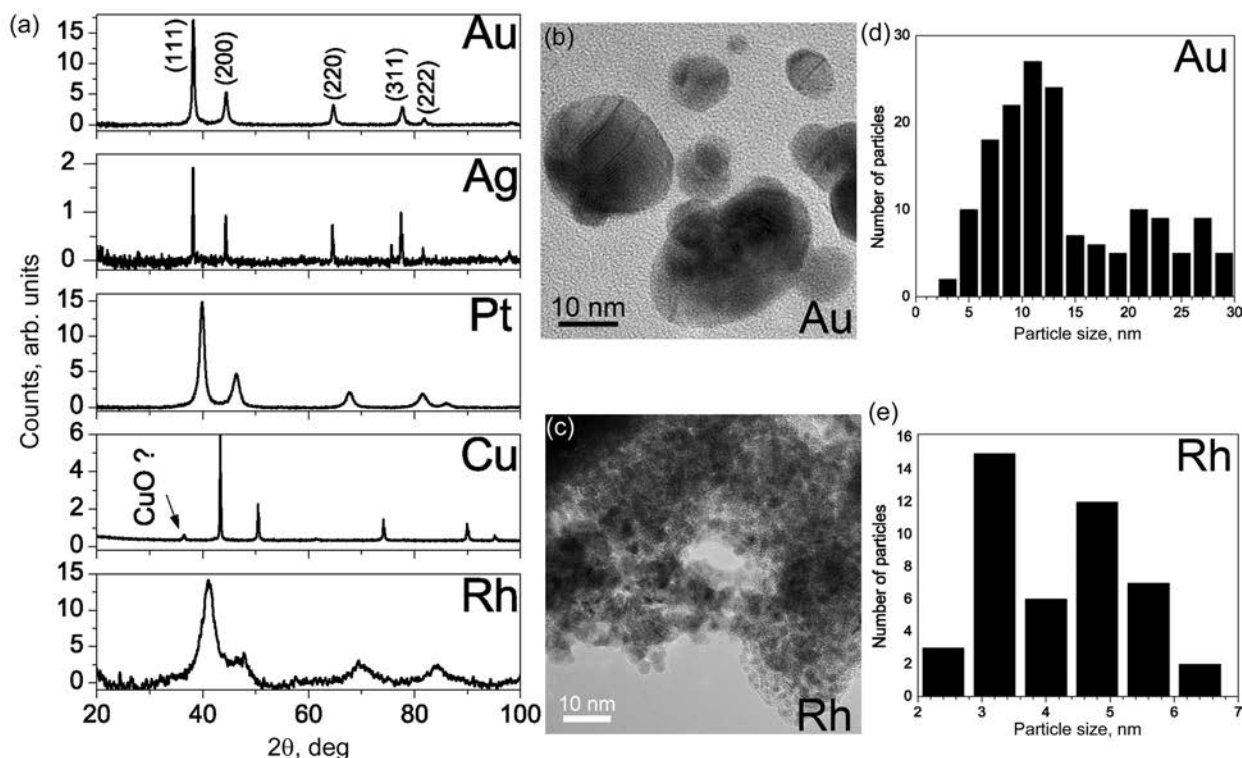


Fig. 5. (a) X-ray diffraction patterns of Au, Ag, Pt, Cu and Rh nanoparticles produced by ac corrosion in NaOH. The positions of the peaks coincide with those expected for the crystal structure of a corresponding metal (in the case of Cu and perhaps Ag some oxide is also visible). Using Scherrer formula, which correlates the width of a diffraction line to the crystallite size in the sample, we obtain the rough indication for the average crystallite size to be 15, 58, 12, 57 and 6 nm, respectively\*. (b), (c) TEM images of Au and Rh nanoparticles, respectively. (d), (e) Size distributions of Au and Rh nanoparticles, obtained from the analysis of the TEM images.

\* The value for Au was recently revised through better fitting and comprehensive data analysis.

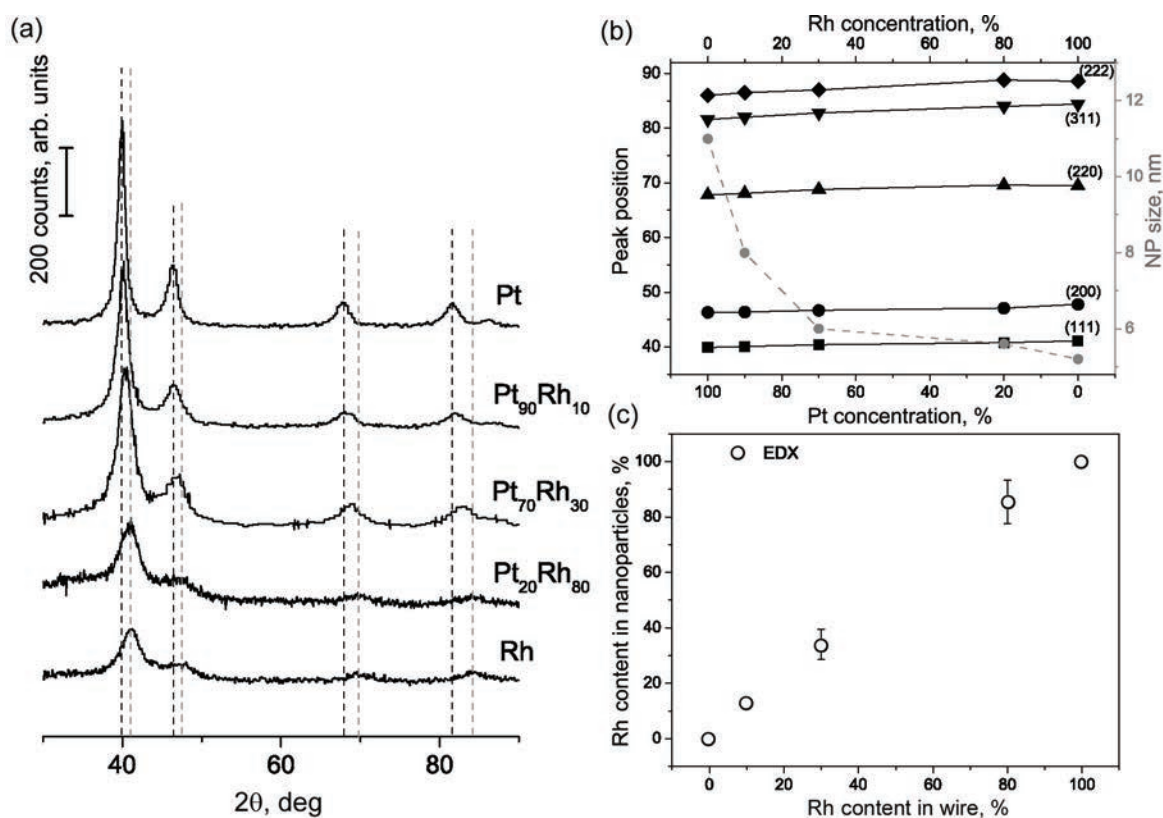


Fig. 6. (a) XRD patterns of the nanoparticles obtained from Pt<sub>x</sub>Rh<sub>1-x</sub> alloys of different composition. Dashed lines indicate positions of pure Pt (black) and Rh (grey) diffraction maxima. (b) Position of the diffraction lines vs. the composition of the alloy. Grey, dashed line shows the resulting average particle size per alloy. (c) Energy dispersive x-ray (EDX) analysis of the composition of the Pt<sub>x</sub>Rh<sub>1-x</sub> nanoparticles. Reproduced from Ref. 16.

The data presented above convincingly shows that cathodic corrosion is not an exclusive property of platinum, and that other metals also readily form nanoparticles under these electrochemical conditions. It is now tempting to see what would happen if the starting electrode wire is made of an alloy. In the following we show that in this case the nanoparticles retain the alloy's composition. Our XRD results for a series of platinum–rhodium alloys, presented in Fig. 6(a), reveal a surprisingly good agreement with the Vegard rule [15]: the lattice constant, determined from the position of the diffraction lines, changes linearly between the limiting values of two pure metals proportionally to their concentration in the alloy, see Fig. 6(b). An independent EDX analysis reveals a very similar composition of the nanoparticles, see Fig. 6(c). This is a rather important result, as it not only shows that the composition of the alloy is retained in the nanoparticles, but also that the constituent metals in the nanoparticles do not segregate but remain properly alloyed.

The PtRh alloy example is not unique — other alloys also exhibit similar behavior, see Fig. 7 [16]. This shows that the cathodic corrosion method provides an easy way to synthesize alloy nanoparticles.

To summarize, the cathodic corrosion method of nanoparticle synthesis allows one to produce clean particles of

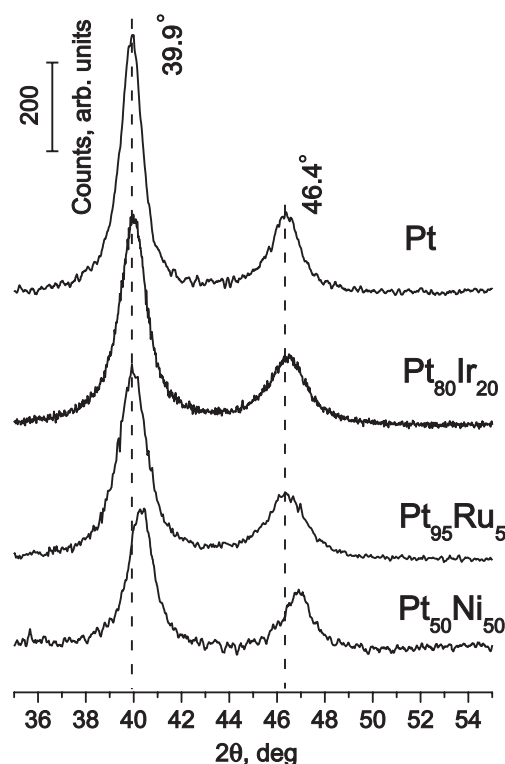


Fig. 7. XRD patterns of nanoparticles of some platinum alloys. The shift of the diffraction lines from the pure Pt positions (dashed lines) is the consequence of alloying.

virtually any metal. The nanoparticles have a narrow size distribution and the average particle size can be easily controlled. Furthermore, if the starting electrode is an alloy, the method yields alloyed nanoparticles. Finally, there appear to be further possibilities towards controlling the surface termination and thus the shape of the nanoparticles.

### Catalytic properties

All these properties are particularly attractive for applications in heterogeneous catalysis. Platinum, being one of the most scarce and expensive metals, is also one of the best industrial catalysts. As the reactions take place only on the surface of platinum, it is extremely advantageous to maximize its surface area by converting platinum into nanoparticles. Additionally, catalytic activity of small nanoparticles may be enhanced due to size-effects [1]. We have shown that platinum nanoparticles synthesized by the cathodic corrosion method show higher catalytic activity per gram of platinum than the state-of-the-art commercial catalysts. This is due to the fact that the surface of our nanoparticles is extremely clean and, since they are formed in highly non-equilibrium conditions, has many irregularities known as "active sites" [14]. The latter are especially advantageous for the oxidation reactions of small alcohols, relevant for fuel cells [1].

Another catalytic process that is very relevant for wastewater treatment is the reduction of nitrite (or nitrate) to nitrogen. While most processes reduce nitrite to ammonia, recently an electrochemical process has been discovered which can very selectively convert nitrite into dinitrogen [17]. Unfortunately, the selectivity can only be obtained on Pt(100) single crystal electrodes, which is clearly an impractical solution for removing nitrite contamination from wastewater. By synthesizing platinum nanoparticles with high amount of (100) sites on the surface as described above, we have managed to obtain the required selectivity also on the practical nanocatalyst.

In industrial catalysis it is long established that alloys often have superior catalytic properties compared to pure metals. For example PtRu alloy is much more resistant to carbon monoxide poisoning in an alcohol fuel cell compared to pure Pt [18]. The combination of Pt and Rh in an alloy should be advantageous for nitrate reduction. With the cathodic corrosion method we have synthesized both the PtRu and PtRh nanoparticles and showed their enhanced activity for methanol oxidation and nitrate reduction, respectively [16]. In the future it would be most interesting to apply this method to the synthesis of the automotive three-way exhaust catalyst, which consists of Pt, Rh and Pd.

### Conclusions

In this article we have presented a new, simple yet versatile method for the electrochemical synthesis of nanoparticles. We have also shown that this new method allows for great control of their properties, namely the size, the shape and the composition. As these are the very first results, we envisage many more possibilities for making practical quantities of nanoparticles with pre-defined properties using this method of cathodic corrosion.

One attractive possibility, briefly mentioned in the text, is the synthesis of bimetallic nanoparticles where one metal will oxidize, providing an oxidic support for a catalytic nanoparticle of the second metal. This will provide great flexibility towards synthesizing novel catalysts for numerous reactions. Another yet unexplored possibility lies in using this method for the synthesis of semiconductor nanocrystals, also known as quantum dots. Further, one can think of exploiting the universality of the method for the synthesis of, e.g., superconducting (alloy) nanoparticles, etc. It is clear that both the fundamental aspects of novel chemistry of cathodic corrosion and the broad horizon of potential applications should be explored further.

### Acknowledgments

A.I.Y. and Yu.I.Y. acknowledge the Dutch NWO vidi grant and STW Valorization grant (project 12572), respectively. We thank P. Rodriguez for his pioneering contribution to the (100)-terminated nanoparticle studies, F. Tichelaar and P. Kooyman (TU Delft) for TEM analysis, E. Bouwman for providing generous access to the XRD facility.

1. M.T.M. Koper, *Nanoscale* **3**, 2054 (2011).
2. Yu.I. Yanson and A.I. Yanson, *Fiz. Nizk. Temp.* **39**, 390 (2013) [*Low Temp. Phys.* **39**, No. 3 (2013)].
3. N.F.M.K. Henry, H. Lipson, and W.A. Wooster, *The Interpretation of X-ray Diffraction Photographs*, MacMillan, London (1960).
4. H.J. Wasserman and J.S. Vermaak, *Surf. Sci.* **32**, 168 (1972).
5. C. Solliard and M. Flueli, *Surf. Sci.* **156**, 487 (1985).
6. N. Tian, Z.Y. Zhou, S.G. Sun, Y. Ding, and Z.L. Wang, *Science* **316**, 732 (2007).
7. S. Link and M.A. El-Sayed, *J. Phys. Chem. B* **103**, 8410 (1999).
8. F.J. Vidal-Iglesias, J. Solla-Gullon, P. Rodriguez, E. Herrero, V. Montiel, J.M. Feliu, and A. Aldaz, *Electrochem. Commun.* **6**, 1080 (2004).
9. A. Rodes, K. Elachi, M.A. Zamakhchari, and J. Clavilier, *J. Electroanal. Chem.* **284**, 245 (1990).
10. J. Solla-Gullon, P. Rodriguez, E. Herrero, A. Aldaz, and J.M. Feliu, *Phys. Chem. Chem. Phys.* **10**, 1359 (2008).
11. J. Solla-Gullon, A. Rodes, V. Montiel, A. Aldaz, and J. Clavilier, *J. Electroanal. Chem.* **554**, 273 (2003).
12. F. Calle-Valejo, *private communication*.

13. S. Trasatti and O.A. Petrii, *J. Electroanal. Chem.* **327**, 353 (1992).
14. A.I. Yanson, P. Rodriguez, N. Garcia-Araez, R.V. Mom, F.D. Tichelaar, and M.T.M. Koper, *Angew Chem. Int. Edit.* **50**, 6346 (2011).
15. A.R. Denton and N.W. Ashcroft, *Phys. Rev. A* **43**, 3161 (1991).
16. P. Rodriguez, F.D. Tichelaar, M.T.M. Koper, and A.I. Yanson, *J. Am. Chem. Soc.* **133**, 17626 (2011).
17. M. Duca, M.O. Cucarella, P. Rodriguez, and M.T. M. Koper, *J. Am. Chem. Soc.* **132**, 18042 (2010).
18. H.A. Gasteiger, N. Markovic, P.N. Ross, and E.J. Cairns, *J. Phys. Chem.* **97**, 12020 (1993).